Lawrence Berkeley National Laboratory

Recent Work

Title

Infrared Spectroscopy of the Molecular Hydrogen Solvated Carbonium Ions, CH{sub 5 sup +} (H{sub 2)}{sub n} ((N = 1 - 6)

Permalink

https://escholarship.org/uc/item/36t5f1h8

Journal

Journal of Chemical Physics, 103(2)

Authors

Boo, D.W.
Lee, Yuan T.

Publication Date

1995-02-01

eScholarship.org Powered by the California Digital Library
University of California

LBL-36834
UC-401
Preprint

Lawrence Berkeley Laboratory
UNIVERSITY OF CALIFORNIA

CHEMICAL SCIENCES DIVISION

Submitted to Journal of Chemical Physics

Infrared Spectroscopy of the Molecular Hydrogen Solvated Carbonium Ions, $CH_5^+(H_2)_n$ (n = 1 – 6)

D.W. Boo and Y.T. Lee

February 1995

REFERENCE COPY
Does Not
Circulate
Bldg. 50 Library.
LBL-36834
Copy 1

Prepared for the U.S. Department of Energy under Contract Number DE-AC03-76SF00098

DISCLAIMER

This document was prepared as an account of work sponsored by the United States Government. While this document is believed to contain correct information, neither the United States Government nor any agency thereof, nor the Regents of the University of California, nor any of their employees, makes any warranty, express or implied, or assumes any legal responsibility for the accuracy, completeness, or usefulness of any information, apparatus, product, or process disclosed, or represents that its use would not infringe privately owned rights. Reference herein to any specific commercial product, process, or service by its trade name, trademark, manufacturer, or otherwise, does not necessarily constitute or imply its endorsement, recommendation, or favoring by the United States Government or any agency thereof, or the Regents of the University of California. The views and opinions of authors expressed herein do not necessarily state or reflect those of the United States Government or any agency thereof or the Regents of the University of California.

LBL-36834
UC-401

Infrared Spectroscopy of the Molecular Hydrogen Solvated Carbonium Ions, $CH_5^+(H_2)_n$ (n = 1 – 6)

Doo Wan Boo and Yuan T. Lee

Department of Chemistry
University of California, Berkeley

and

Chemical Sciences Division
Lawrence Berkeley Laboratory
University of California
Berkeley, California 94720

February 1995

This work was supported by the Director, Office of Energy Research, Office of Basic Energy Sciences, Chemical Sciences Division, of the U.S. Department of Energy under Contract No. DE-AC03-76SF00098.

Infrared Spectroscopy of the Molecular Hydrogen Solvated Carbonium Ions, $CH_5^+(H_2)_n$ (n = 1 - 6)

Doo Wan Boo and Yuan T. Lee
Department of Chemistry, University of California, Berkeley, CA 94720, USA
and Chemical Sciences Division, Lawrence Berkeley Laboratory, 1 Cyclotron Road, Berkeley, CA 94720, USA

ABSTRACT

The infrared spectra for the molecular hydrogen-solvated carbonium ions, $CH_5^+(H_2)_n$ (n=1- 6) in the frequency range of 2700-4200 cm^{-1} are presented. Spectroscopic evidence was found in support of the scrambling of CH_5^+ through the large amplitude motions such as the CH_3 internal rotation and the in-plane wagging motion of three-center two-electron bond. More importantly, the scrambling motions of CH_5^+ cores were slowed down considerably by attaching the solvent H_2 molecules to the core ion. The complete freezing of the scrambling motions was found when the first three H_2 molecules were bound to the CH_5^+ core. A good agreement between the experimental and the theoretical predictions was found in the dynamics of CH_5^+.

1. INTRODUCTION

Protonated alkanes are highly reactive intermediates in the acid-catalyzed transformations of hydrocarbons.[1] These nonclassical carbonium ions are known to form a three-center two-electron (3c2e) bond having pentacoordinated carbon atoms and bridged hydrogens.[2] CH_5^+ is the simplest carbonium ion.

The existence of CH_5^+ was first reported by Tal'roze and Lyubinova in mass spectrometric studies on the protonation of alkenes and alkanes in 1952.[3] Olah and coworkers later reported that CH_5^+ played an important role as a reactive intermediate in super acid solution reactions.[4] CH_5^+ is now used as a common reagent for protonation of gas phase molecules in the chemical ionization mass spectrometry.[5] It is also of astrophysical interest in that it may play as an intermediate for generation of methane and formaldehyde in the cold galactic molecular clouds.[6]

A number of the early theoretical calculations on the structures of CH_5^+ consistently suggested that the eclipsed C_s (e-C_s) symmetry structure was the global minimum energy structure.[7-10] However, recent ab initio calculations at the most sophisticated level, performed by Schleyer, Schaefer, and coworkers, found that the energy differences between the e-C_s structure and other structures such as staggered C_s (s-C_s) or C_{2v} were very small and became negligible when corrected for zero point energies (see Fig. 1 for the CH_5^+ structures).[11,12] The C_{4v} and D_{3h} structures were predicted to be higher in energy than the e-C_s structure by 1 kcal/mole and 9 kcal/mole, respectively. As pointed out by Schleyer, Schaefer, and later, by Scuceria,[13] the early prediction that CH_5^+ is regarded as a complex between CH_3^+ and H_2 with a localized 3c2e bond is not valid, but CH_5^+ is likely to scramble constantly through the low lying s-C_s and C_{2v} transition states, without possessing a definite equilibrium structure.

In contrast to the numerous theoretical works on CH_5^+, only a few experiments have been performed previously to characterize indirectly the structure of CH_5^+ using mass spectrometry.[14-18] Hiraoka and coworkers measured $\Delta H°_{n-1,n}$ and $\Delta S°_{n-1,n}$ for the clustering reactions $CH_5^+(CH_4)_{n-1} + CH_4 = CH_5^+(CH_4)_n$ for n=1-9 using a pulsed electron beam mass spectrometry.[14] They showed an irregular decrease in the values of $-\Delta H°_{n-1,n}$ and $-\Delta S°_{n-1,n}$ between n=2 and 3, suggesting a C_s symmetry structure for CH_5^+ which contains a 3c2e bond, since the two acidic H atoms of the 3c2e bond would give the most favorable sites for the first two CH_4 ligands. However, this result

only suggests the C_s structure for the core ion CH_5^+ of $CH_5^+(CH_4)_n$, not for free CH_5^+, because strong interaction between CH_5^+ and CH_4 could deform the structure of free CH_5^+ ($\Delta H^\circ_{0,1}$=6.87 kcal/mole). In order to get more reliable information on the structure of CH_5^+, they also measured $\Delta H^\circ_{n-1,n}$ and $\Delta S^\circ_{n-1,n}$ for the cluster ions $CH_5^+(H_2)_n$ (n=1-4), which were expected to have much weaker interactions between the core ion CH_5^+ and H_2 molecules.[15] Unlike the case for $CH_5^+(CH_4)_n$, a gradual decrease of $\Delta H^\circ_{n-1,n}$ with n was observed for $CH_5^+(H_2)_n$, though a large gap in the van't Hoff plots was still seen between n=2 and 3. Based upon these observations, they proposed that CH_5^+ still has C_s structure but the positive charge is more delocalized in CH_5^+ when it is complexed by H_2.

Experiments using a Fourier Transform Ion Cyclotron Resonance (FTICR) mass spectrometry have been performed on the collisionally induced intramolecular randomization of hydrogen and deuterium atoms in CH_4D^+ and CD_4H^+ by the groups of Sefcik's,[16] Smith's,[17] and Heck's.[18] In these works, the product ion branching ratio $[BH^+]/[BD^+]$ associated with the proton/deuteron transfer reaction from CH_4D^+ and CD_4H^+ to the base B was measured as a function of the average number (<n>) of primary ion/molecule collisions ($CH_4^{+\cdot}/CD_4$ or $CD_4^{+\cdot}/CH_4$). The idea of these studies was that if significant potential barriers exist for the scrambling motions of CH_5^+, the D atom in CH_4D^+ and the H atom in CD_4H^+ would be located at one of the two H atoms forming a 3c2e bond in the C_s structure, and the branching ratio will be 1:1 for both CH_4D^+ and CD_4H^+cases (C_s model). If small or no barriers exist for the scrambling motions, the branching ratio will be 4:1 and 1:4 for CH_4D^+ and CD_4H^+ cases, respectively (randomized model). However, the results were inconsistent in that Sefcik's[16] and Heck's results[18] supported the C_s model with a localized 3c2e bond whereas Smith's results[17] suggested the randomized model.

Because of the difficulties in the indirect characterization of the structure of CH_5^+, much effort has been given to obtain high resolution infrared (IR) spectra for CH_5^+, but has achieved little success. One of the difficulties in the high resolution IR study is that CH_5^+ scrambles even at low temperatures, as predicted by the ab initio calculations, causing significant spectral congestion. The spectral congestion would be more extensive for the CH_5^+ ions produced in the conventional ion sources since the ions tend to possess considerable internal energy.

In an attempt to overcome the difficulties of performing IR spectroscopy on CH_5^+, we

have studied the molecular hydrogen solvated carbonium ions, $CH_5^+(H_2)_n$ (n=1-6) where the H_2 molecules are weakly bound to the core ion. The motivation was the notion that the interactions between the core CH_5^+ ions and the H_2 molecules are weak enough to cause only a minor perturbation to CH_5^+, yet strong enough to slow down the scrambling motions. According to Hiraoka and coworkers, the binding energies ($\Delta H_{n-1,n}$) of the H_2 molecules to the CH_5^+ core were measured to be less than 2 kcal/mole.[15] Schaefer and coworkers also calculated the dissociation energy (D_0) of $CH_5^+(H_2)$ to be 1.46 kcal/mole at TZ2P+d CCSD(T).[19] The experimental and theoretical dissociation energies and enthalpies for $CH_5^+(H_2)_n$ (n=1-4) are listed in Table I. Experimentally, the weakly bound clusters $CH_5^+(H_2)_n$ have advantages over CH_5^+ in that the cooling of the cluster ions by supersonic expansion is more efficient than the cooling of the CH_5^+ ions, since the low frequency modes involving the core-ligand bonds would play an important role in the vibrational energy transfer from initially hot ions to the cold partners. As a preliminary result, the IR spectra for $CH_5^+(H_2)$ have been reported previously.[20]

Very recently, we also reported a study on the dynamics of the molecular hydrogen solvated carbonium ions, $CH_5^+(H_2)_n$ (n=1,2,3) by measuring the IR spectra for the C- H stretching modes of $CH_5^+(H_2)_n$ (n=1,2,3), and performing ab initio molecular dynamics (MD) simulations on $CH_5^+(H_2)_n$ (n=0-3).[21] The results provided considerable insight into the scrambling motion of CH_5^+, and revealed the slowdown of the scrambling of the CH_5^+ core by the solvent H_2 molecules in $CH_5^+(H_2)_n$ (n=1,2,3).

In this paper, we present the complete IR spectra of the molecular hydrogen solvated carbonium ions, $CH_5^+(H_2)_n$ (n=1-6) including the IR spectra for the H-H stretching modes of the solvent H_2 molecules, obtained in the frequency range of 2700- 4200 cm^{-1}. It will be shown that correlation of the spectral features for the C-H stretching modes of the core CH_5^+ with the number of solvent H_2 molecules in $CH_5^+(H_2)_n$ (n=1-6) can provide information on the structure and dynamics of CH_5^+. It will also be shown that the vibration-rotation transitions of the H-H stretching modes in $CH_5^+(H_2)_n$ (n=1-6) can give additional information on the structure and dynamics of CH_5^+ as well as information about the interactions between the CH_5^+ core and the solvent H_2 molecules.

2. EXPERIMENTAL DETAILS

The experimental apparatus used in this work has been described previously.[22-26] A schematic of the machine is given in Fig. 2. Briefly, the molecular hydrogen solvated carbonium ions $CH_5^+(H_2)_n$(n=1-6) were produced from a high pressure corona discharge source and subsequent supersonic expansion through a 75 μm nozzle. A schematic of the corona discharge ion source is shown in Fig. 3. The corona discharge was maintained in 50-150 torr of gas with ultrahigh purity (UHP) H_2 and UHP CH_4 in a 3,000,000 : 1 ratio, flowing past a 1.0 kV potential from the discharge tip of the needle to the source body maintained at approximately 350 V above ground. The discharge current under these conditions was 10 ~ 40 μA. The source was maintained at the optimum temperature for each kind of cluster ion in order to maximize the ion intensity, by heating up the source body cooled by contact with a liquid nitrogen reservoir. Typical source temperatures for the molecular hydrogen solvated carbonium ions were between -20°C and -70°C. Pressures in the source chamber were between $1x10^{-5}$ and $1x10^{-4}$ torr during the experiment. To prevent the acceleration of ions in the higher pressure region, which causes internal excitation and dissociation of the ion clusters via collisions with the background gas, the potential of the skimmer was maintained within 1 V of that of the source body.

After the skimmer, the ion beam entered a second differential pumping region containing collimating and focusing lenses. The pressure in this region was typically an order of magnitude lower than that of the source region. The beam was directed into a 60° sector magnet mass analyzer through a third differentially pumped region maintained at 10^{-8} torr.

The mass-selected beam was then bent 90° in a dc quadrupole field, decelerated to less than 0.5 eV, and focused into a rf octapole ion trap through an entrance aperture lens. The ions were usually trapped here for ~ 2 msec before IR irradiation. Usually, 100 - 500 ions were trapped per cycle, depending upon the stabilities of the cluster ions. These numbers are too small to allow direct measurement of photon absorption.

The trapped, mass-selected clusters were then vibrationally excited by a pulsed, tunable infrared laser. A Quanta-Ray IR WEX was used as a tunable IR light source. The IR wavelength was produced in a $LiNbO_3$ crystal that generates the difference frequency between a Lambda Physics pulsed dye laser (Model FL3002E) and the 1.06 μm fundamental of a

Continuum Nd-YAG laser. The IR bandwidth was 0.2 cm^{-1}. The pulse duration was 6 nsec with a 20 Hz repetition rate, and the laser power was 1-3 mJ/pulse in the 2700-4200 cm^{-1} frequency region scanned in this work.

If the ions absorb one IR photon in the tuning range of 2700-4200 cm^{-1}, the $CH_5^+(H_2)_n$ (n=1-6) ions vibrationally predissociate into $CH_5^+(H_2)_x + yH_2$ (x+y=n). Large cluster ions are so weakly bound that the vibrational predissociation of these ions can produce two or more daughter ions which differ by the mass of H_2. Roughly 0.5 msec after the laser pulse, the potential on the exit aperture was lowered to extract ions of all masses from the trap. These ions were filtered by a quadrupole mass spectrometer tuned to pass only the daughter ions $CH_5^+(H_2)_x$. The observation of the $CH_5^+(H_2)_x$ signal as a function of laser frequency was a measure of the IR absorption of $CH_5^+(H_2)_n$ (n=1-6).

Daughter ions were counted with a Daly ion detector[27] for each laser shot. Background daughter ions resulting from the decay of metastable parent ions in the rf ion trap were monitored in a separate cycle with the laser off at each wavelength and subtracted from the laser on signal. The laser power was monitored at each data point, and spectra were normalized for the power of the tunable IR laser assuming a simple linear power dependence. For a typical experiment, signals were averaged for about 500 laser shots for $CH_5^+(H_2)_n$(n=1-6) at each wavelength in the 2700-3200 cm^{-1} and 4000-4150 cm^{-1} frequency regions, where the IR absorptions were found for $CH_5^+(H_2)_n$ (n=1- 6).

In this experiment, the composition of ions in the beam was strongly dependent on the H_2/CH_4 mixing ratios, source temperatures and source pressures. The experimental conditions used in this work were a H_2:CH_4 ratio of 3,000,000:1, a source temperature of -30°C and a source pressure of 60-150 torr. Fig. 4 shows the mass spectrum for $CH_5^+(H_2)_n$ (n=1-6) obtained under these conditions. The mass spectrum shows a Gaussian distribution of the $CH_5^+(H_2)_n$ ions with the cluster size ranging from n=1 to n=6. For the cluster ions with n≥6, the mass peaks were overlapped with the intense peaks due to $C_2H_5^+$ (m/e=29), $C_2H_7^+$ (m/e=31), and $CH_5^+(CH_4)$ (m/e=33). In this experiment, the maximum in the distribution of mass peaks was able to be easily shifted between n=1 and n=6 by changing the source pressures and source temperatures. The maximum ion intensities for large cluster ions were obtained when high source pressures and low source temperatures were used in the discharge.

As reported previously,[20] the $CH_5^+(H_2)$ ions were also produced using a H_2:CH_4 ratio of 2000:1, a -40°C source temperature and 150 torr source pressure. But, the IR spectra obtained with these two different conditions were similar to each other. The IR spectra of $CH_5^+(H_2)$ obtained with the latter conditions is presented in this paper, simply because of the superior signal-to-noise ratio.

3. RESULTS AND ANALYSIS

3.1 Internally Cold $CH_5^+(H_2)_n$ Ions

Since CH_5^+ is expected to scramble extensively even at the moderate temperatures, it is crucial to produce the ions in internally cold forms in order to obtain information about the structure and dynamics of the CH_5^+ cores in the molecular hydrogen solvated carbonium ions, $CH_5^+(H_2)_n$ (n=1-6). Therefore, it seems appropriate to discuss the conditions of the carbonium ions (CH_5^+ and $CH_5^+(H_2)_n$) produced in this experiment. As described in detail in the previous section, the carbonium ions were produced in a high pressure and low current corona discharge source and subsequent supersonic expansion. The ionization conditions were kept as soft as possible at the sacrifice of the ion intensity. Nevertheless, the carbonium ions were likely to be vibrationally excited by the discharge process, and were expected to cool down via collisions with cold neutral species in a small high pressure drift region and during supersonic expansion. It is well known that the collisional cooling strongly depends upon the efficiency of energy transfer from internally hot ions to the cold partners. If the cold partners (e.g. CH_4) possess similar vibrational frequencies as the internally hot ions, the ions would be cooled much more efficiently by the mechanism of resonant energy transfer. However, this mechanism may not be significant in the cooling process of the ions produced in this work, since the concentration of methane in the gas mixture was kept low in order to avoid the formation of larger hydrocarbon ions. Large hydrocarbon ions such as $C_2H_3^+$, $C_2H_5^+$, $C_3H_7^+$, and $C_4H_9^+$, instead of the carbonium ions, were found to be dominant in the mass spectrum when the concentration of methane was high (see ref. 26 for the details). Therefore, the primary mechanism for the cooling of the carbonium ions in this work would be nonresonant energy transfer, efficient only when the molecules possess low frequency vibrational modes.

According to the ab initio calculations on CH_5^+ and $CH_5^+(H_2)$,[11,19] the lowest vibrational frequency for e-C_s CH_5^+ was predicted to be quite high (856 cm^{-1}) since the CH_3-H_2 torsional mode (145 cm^{-1}) would be a free internal rotation. On the other hand, the molecular hydrogen solvated carbonium ions, $CH_5^+(H_2)_n$ were predicted to possess several low frequency modes involving the core-ligand bonds. As a result, the CH_5^+ ions were expected to possess significant internal energy due to the inefficient cooling whereas the $CH_5^+(H_2)_n$ (n=1-6) ions were expected

to be internally cold. Besides, if $CH_5^+(H_2)_n$ ions contain more internal energy than the solvation energy, it will dissociate and produce cooler ions.

Internally cold small clusters of $CH_5^+(H_2)_n$ could also be formed during the flight before the mass selection in the magnetic sector, by releasing some H_2 molecules from the large clusters of $CH_5^+(H_2)_n$. The $CH_5^+(H_2)_n$ (n=1-6) ions were further cooled down by storing them in an ion trap for ~2 msec, during which some radiative cooling took place. Metastable ions, if they exist, would dissociate during the trapping time, and their contributions to the observed IR spectra were eliminated by doing a background substraction with the experimental scheme of laser on and off. In this experiment, the background level with laser off was found to be less than 0.1 % of the parent ions, indicating the cold nature of the molecular hydrogen solvated carbonium ions, $CH_5^+(H_2)_n$ (n=1-6).

3.2 Infrared Spectra

Fig. 5 shows the IR spectra for the molecular hydrogen solvated carbonium ions, $CH_5^+(H_2)_n$ (n=1-5) obtained in the frequency range of 2700-3200 cm^{-1}. The spectral features in this frequency region are due to the C-H stretching modes of the CH_5^+ cores in $CH_5^+(H_2)_n$ (n=1-5). Three C-H stretching bands were predicted by ab initio calculations in this frequency range, and the solid lines in Fig. 5 are the result of a least squares fit with three gaussian peaks. The positions of the fitted gaussian peaks are listed in Table III.

Fig. 6 shows the IR spectra for the molecular hydrogen solvated carbonium ions $CH_5^+(H_2)_n$ (n=1-6) obtained in the frequency range of 4050-4150 cm^{-1}. The observed features are due to the H-H stretching modes of the solvent H_2 molecules in $CH_5^+(H_2)_n$ (n=1-6).

In this work, the signal-to-noise ratios of the IR spectra for the large clusters were found to be considerably lower than those for the small clusters, since the absolute number densities of the large clusters were found to be lower than the small clusters due to the weaker binding of the large clusters, and several vibrational predissociation channels available for the large clusters would compete each other, resulting in the smaller number of daughter ions at each channel.

$CH_5^+(H_2)$

The IR spectra for the C-H stretching modes of $CH_5^+(H_2)$, shown in Fig. 5A and 5B, were

obtained by monitoring the CH_5^+ signal (m/e=17). As reported previously,[20,21] the two IR spectra (Fig. 5A and 5B) were obtained with hot ion conditions and cold ion conditions, respectively (see ref. 20 for the details of the source conditions). One broad feature with shoulders, centered at 2964 cm^{-1}, was observed in the IR spectrum with cold ion conditions (Fig. 5B), indicating the floppy nature of CH_5^+. The shoulder features observed in the cold ion spectrum almost disappeared in the hot ion spectrum (Fig. 5A), revealing increased scrambling of the core CH_5^+. The lowest frequency peak among three gaussian peaks fitted into the observed IR spectrum with cold ion conditions was quite broad, extending from 2700 cm^{-1} to 3100 cm^{-1}, centered at 2907 cm^{-1} (see Table III).

According to the recent ab initio calculation on $CH_5^+(H_2)$,[19] three C-H stretching frequencies for e-C_s CH_5^+ core, the global minimum energy structure, were predicted to be 2898, 2998, and 3081 cm^{-1}, corresponding to the symmetric CH_3 breathing, symmetric CH_3 degenerate stretching, and asymmetric CH_3 stretching modes, as shown in Table II. These vibrational modes were also predicted to have more or less similar IR intensities. The C-H stretching frequencies for the low lying transition state structures such as s- C_s and C_{2v} CH_5^+ were predicted to be 2914, 2968, and 3085 cm^{-1} for the former, and 2732, 2987, and 3094 cm^{-1} for the latter (Table II).[11] The two structures were regarded as the transition states along the internal CH_3 rotation, and along the in-plane wagging of the H2 between H1 and H3 in the CH_5^+ core, respectively (see Fig. 1). The latter motion will be referred to subsequently as the in-plane wagging motion. It is interesting to notice that the vibrational assignments for the two high C-H stretching frequencies of s-C_s CH_5^+ core (2968 and 3085 cm^{-1}) were the asymmetric CH_3 stretching and symmetric CH_3 degenerate stretching modes, respectively, which were switched in order, compared to the case for e-C_s CH_5^+. This could be the result of the substantial geometrical changes in the CH_3 group during the internal rotation, as expected from the differences in the optimized C-H bond lengths and angles[11,12] between e-C_s CH_5^+ and s-C_s CH_5^+. This suggests that the vibrational modes involving the three C-H bonds could be strongly coupled to each other via the CH_3 internal rotation.

On the other hand, the C_{2v} CH_5^+ structure consisted of two strong C-H bonds and three weak C-H bonds forming a four-center three electron (4c3e) bond. Correspondingly, the three C-H stretching frequencies (2732, 2987, and 3094 cm^{-1}) were assigned to the asymmetric C-H

stretching mode involving two weak C-H bonds, symmetric and asymmetric C-H stretching modes involving two strong C-H bonds, respectively (Table II).[11] The 2732 cm^{-1} mode, strongly red-shifted from the other two C-H stretching modes of the C_{2v} structure, were distinct from the C-H stretching modes of the C_s (e-C_s and s-C_s) structures, and could play as an indicator of the scrambling of CH_5^+ via the in-plane wagging motion involing the C_{2v} transition state.

The observation of one broad feature with shoulders in the IR spectrum (Fig. 5B) and the result of the broad gaussian peak fitted into the low frequency shoulder, contributed from the C_{2v} structure, suggested that the CH_5^+ core in $CH_5^+(H_2)$ scrambles considerably via large amplitude motions such as the CH_3 internal rotation involving the s-C_s transition state, and the in-plane wagging motion involving the C_{2v} transition state. Nonetheless, the center of the observed feature at 2965 cm^{-1} was only 27 cm^{-1} red-shifted from the average C-H stretching frequency of CH_4 (2992 cm^{-1}),[28] reflecting the fact that when a hydrogen atom in CH_5^+ does not participate in the scrambling motions, its corresponding C-H bond is similar to the C-H bond in CH_4.

Fig. 6A shows the IR spectrum for the H-H stretching mode of the H_2 in $CH_5^+(H_2)$, obtained by monitoring the CH_5^+ signal (m/e=17) with 0.2 cm^{-1} laser resolution. The vibration-rotational spectrum shows clear P-, Q-, and R-branches, indicating the A-type transition of a near symmetric top. The band origin was 4077.4 cm^{-1}, 82.6 cm^{-1} red-shifted from free H_2 (4160 cm^{-1}), which suggests that the interaction between the CH_5^+ core and the H_2 molecule in $CH_5^+(H_2)$ is dominated by the electrostatic charge-induced dipole interaction. The dipole moment of H_2 induced by the ion core allowed the H-H stretching mode to be IR active. The spacing of adjacent rotational lines ranged from 1.4 cm^{-1} to 1.6 cm^{-1}. The rotational lines were found to possess some fine structures, as shown in Fig. 6A. Two anomalously intense peaks were observed in the R-branch side, as indicated by asterisks in Fig. 6A, and they could be assigned to the Q-branches of two hot band transitions. The rotational progressions of the hot band transitions may contribute to the wide spread of rotational lines with a high background, observed in the R-branch side (see Fig. 6A). The full analysis of the vibration-rotational spectrum will be reported elsewhere.

$CH_5^+(H_2)_2$

Fig. 5C shows the IR spectrum for the C-H stretching modes of $CH_5^+(H_2)_2$, obtained by

monitoring the CH_5^+ signal (m/e=17). Two spectral features, centered at 2957 cm^{-1} and 3078 cm^{-1}, were observed in the frequency range of 2700-3200 cm^{-1}. The broad and intense feature at 2957 cm^{-1} was fitted with two equal gaussian peaks centered at 2930 and 2983 cm^{-1}, respectively, as shown in Table III, and the narrow feature at 3078 cm^{-1} was fitted with one gaussian peak. The ab initio C-H stretching frequencies for e-C_s CH_5^+ in $CH_5^+(H_2)_2$, shown in Table II, were more or less similar to those for e-C_s CH_5^+ in $CH_5^+(H_2)$ after appropriate scaling. The ab initio C-H stretching frequencies for s-C_s and C_{2v} CH_5^+ cores in $CH_5^+(H_2)_2$ were also expected to be similar to the corresponding frequencies for $CH_5^+(H_2)$.

The low frequency shoulder feature observed in the IR spectrum for $CH_5^+(H_2)$ was not present in the spectrum for $CH_5^+(H_2)_2$. This suggested that the scrambling motion through the in-plane wagging motion (via C_{2v} structure) may be frozen out by the two H_2 molecules in $CH_5^+(H_2)_2$, unlike the case for $CH_5^+(H_2)$. However, the scrambling of the CH_5^+ core through the CH_3 internal rotation was still extensive, indicated by the broad feature at 2957 cm^{-1}, and strong anharmonic couplings for the vibrational modes involving these three C-H bonds were also expected.

Fig. 6B shows the IR spectrum of the H-H stretching modes for the two H_2 molecules in $CH_5^+(H_2)_2$, obtained by monitoring the CH_5^+ signal in the frequency range of 4050-4150 cm^{-1}. The IR spectrum was taken with 0.2 cm^{-1} laser resolution and 1 cm^{-1} scan step. In spite of the large scan step, the observed spectrum showed clear P-,Q-, and R-branches, indicating the A-type transition of a near symmetric top. The presence of a single rotational progression suggested that the two H_2 molecules were bound to the two H atoms forming a 3c2e bond, with almost equal strength. In this case, the in-phase H-H stretching vibration of the two H_2 molecules would be responsible for the observed feature since the change of dipole moment due to the in-phase vibration would be along the A-axis of $CH_5^+(H_2)_2$.

The band origin was ~4088 cm^{-1}, 72 cm^{-1} red-shifted from free H_2, but 10 cm^{-1} blue-shifted from $CH_5^+(H_2)$. This indicated that the interactions between CH_5^+ core and two H_2 molecules in $CH_5^+(H_2)_2$ were also the charge-induced dipole interactions, and the interactions were weaker for $CH_5^+(H_2)_2$ since the positive charge of the core CH_5^+ was more delocalized in $CH_5^+(H_2)_2$.

$CH_5^+(H_2)_3$

Fig. 5D shows the IR spectrum for the C-H stretching modes of $CH_5^+(H_2)_3$, obtained by monitoring the CH_5^+ signal in the frequency range of 2800-3100 cm^{-1}. Three partially resolved peaks, centered at 2892, 2977, and 3062 cm^{-1}, were found in the IR spectrum. The presence of the three well-separated peaks suggested that the scrambling motions of the CH_5^+ core were almost frozen out by the three H_2 molecules in $CH_5^+(H_2)_3$, and the CH_5^+ core could be considered as semi-rigid. It is interesting to notice that the observed frequencies (2892, 2977, 3062 cm^{-1}) match well with the three ab initio CH_3 stretching frequencies for e-C_s CH_5^+ (2891, 2993, 3079 cm^{-1}) and e-C_s $CH_5^+(H_2)$ (2898, 2998, 3081 cm^{-1}), calculated at TZ2P (+f) CCSD level,[19] as shown in Table II. The ab initio CH_3 stretching frequencies of e-C_s $CH_5^+(H_2)_3$, calculated at MP2/6-311G(D,P) level,[29] also match well with the observed frequencies after appropriate scaling (see Table II). It suggests that the CH_5^+ core in $CH_5^+(H_2)_3$ possesses an e-C_s structure. Since the adiabatic approximations made in the normal mode analysis on the C-H stretching frequencies are expected to be valid due to the semi-rigidity of the CH_5^+ core, the three observed features could be assigned to the symmetric CH_3 breathing, symmetric CH_3 degenerate stretching, and asymmetric CH_3 stretching modes, according to the ab initio normal mode analysis.[19] Furthermore, the new scaling factors for the anharmonic corrections were calculated by the ratio of 2977 cm^{-1}, one of the observed frequencies, to the corresponding ab initio frequency for the e-C_s CH_5^+ core at the level of theory. The rescaled frequencies are listed in the parentheses of Table II.

Fig. 6C shows the IR spectrum for the H-H stretching modes of the three H_2 molecules in $CH_5^+(H_2)_3$, obtained by monitoring the CH_5^+ signal in the frequency range of 4050-4140 cm^{-1}. Unlike the cases for $CH_5^+(H_2)$ and $CH_5^+(H_2)_2$, one broad feature was observed in the spectrum. One of the reasons for the spectral congestion was that the third H_2 molecule in $CH_5^+(H_2)_3$ was bound to the CH_5^+ core in a different environment from the first two H_2 molecules, indicating the presence of a 3c2e bond in the CH_5^+ core in $CH_5^+(H_2)_3$. The center of the broad feature was located at ~4099 cm^{-1}, 61 cm^{-1} red-shifted from free H_2, but 11 cm^{-1} blue-shifted from that of $CH_5^+(H_2)_2$. This also suggested that the interactions of the CH_5^+ core with the H_2 molecules became weaker due to the increased charge delocalization in $CH_5^+(H_2)_3$.

$CH_5^+(H_2)_4$

Fig. 5E shows the IR spectrum for the C-H stretching modes of $CH_5^+(H_2)_4$, obtained by monitoring the CH_5^+ signal. Three peaks, centered at 2878, 2977, and 3067 cm^{-1}, were found in the IR spectrum. These three frequencies were similar to those for $CH_5^+(H_2)_3$ (2892, 2977, and 3062 cm^{-1}), which were assigned to the symmetric CH_3 breathing, symmetric CH_3 degenerate stretching, and asymmetric CH_3 stretching modes, respectively. This result indicated an e-C_s structure for the CH_5^+ core in $CH_5^+(H_2)_4$, but also no significant solvation effect by the fourth H_2 molecule.

Fig. 6D shows the IR spectrum for the H-H stretching modes of the H_2 molecules in $CH_5^+(H_2)_4$. The spectrum was also obtained by monitoring the CH_5^+ signal in the frequency range of 4050-4140 cm^{-1}. One broad feature was again found, centered at ~4106 cm^{-1}, 54 cm^{-1} red-shifted from free H_2, but 7 cm^{-1} blue-shifted from $CH_5^+(H_2)_3$, indicating the weaker interaction due to the increased charge delocalization in $CH_5^+(H_2)_4$. In addition, the slight decrease in the frequency shift from the adjacent smaller cluster (7 cm^{-1} vs 11 cm^{-1}) suggested that the solvent effect on the charge-induced dipole interaction between the hydrogen molecules and the CH_5^+ core started to decrease at n=4, which was consistent with the trend in the C-H stretching bands described above.

$CH_5^+(H_2)_n$ (n=5,6)

Fig. 5F shows the IR spectrum for the C-H stretching modes of $CH_5^+(H_2)_5$. The IR spectrum was obtained by monitoring the $CH_5^+(H_2)$ signal (m/e=19) instead of the CH_5^+ signal, since the $CH_5^+(H_2)$ channel was found to be the major channel for the vibrational predissociation of $CH_5^+(H_2)_5$ in the frequency range of 2700-3200 cm^{-1}. Three features, centered at 2879, 2972, and 3043 cm^{-1}, were found in the spectrum, in spite of the low signal-to-noise ratio. These three frequencies are similar to those for $CH_5^+(H_2)_3$ and $CH_5^+(H_2)_4$, which were assigned to the symmetric CH_3 breathing, symmetric CH_3 degenerate stretching, and asymmetric CH_3 stretching modes of the e-C_s CH_5^+ core, respectively. This suggested that the structure of the CH_5^+ core in $CH_5^+(H_2)_5$ was not changed by the fifth H_2 molecule, but was still an e-C_s structure.

Fig. 6E and 6F show the IR spectra for the H-H stretching modes of $CH_5^+(H_2)_5$ and $CH_5^+(H_2)_6$, respectively. These IR spectra were obtained by monitoring the CH_5^+ signal, the major channel in this frequency region, which was different from the case for the C-H stretching

bands. The additional photon energy in this frequency range was responsible for the complete dissociation. In both spectra, one broad feature was found, centered at 4109 and 4111 cm^{-1}, 51 and 49 cm^{-1} red-shifted from free H_2, respectively. These features were only 3 and 2 cm^{-1} blue-shifted from the adjacent smaller clusters, respectively. This result suggested that the charge induced dipole interactions between the H_2 molecules and the CH_5^+ core were almost in saturation for $CH_5^+(H_2)_5$ and $CH_5^+(H_2)_6$.

4. DISCUSSION

4.1 Dynamics of CH_5^+ in $CH_5^+(H_2)_n$ (n=0-6)

Since the IR spectra for $CH_5^+(H_2)_n$ (n=1-5) provided information about the scrambling motions of CH_5^+ cores, it seems appropriate to discuss the details of the dynamics of CH_5^+ by combining the results of this work and the previous theoretical works. Two crucial theoretical works have been performed previously by Schleyer, Schaefer, and coworkers, and by us in collaboration with Liu and Tse. The first was the high level ab initio calculation at TZ2P+f CCSD level, and the second was the ab initio molecular dynamics (MD) simulation. The two theoretical methods seem to be complementary to each other such that the first provides very accurate electronic energies and harmonic frequencies of CH_5^+, but only for a few optimized nuclear configurations, while the second can simulate all of the classical trajectories of CH_5^+, allowed at the finite temperatures on the ground electronic potential surface, calculated by the density functional method which may not be as accurate as the first.

Both methods predicted the complete scrambling of CH_5^+. According to the high level ab initio calculation,[11,12] the scrambling was predicted to occur through s-C_s and C_{2v} structures, which were regarded as the transition states for the CH_3 internal rotation and the in-plane wagging motion. The two internal motions were expected to be strongly coupled to each other such that the CH_3 internal rotation would be free only when the 3c2e bond involved in the in-plane wagging motion is localized, like in the C_s CH_5^+ structure. The same high level ab initio calculation on $CH_5^+(H_2)$ predicted almost the same results for the CH_5^+ core in $CH_5^+(H_2)$. At present, no high level ab initio calculation has yet been reported on $CH_5^+(H_2)_n$ ($n \geq 2$).

Ab initio MD simulations have been performed on $CH_5^+(H_2)_n$ (n=0-3) as reported previously. During the simulation of ~3 picoseconds at a temperature of ~100K, the 3c2e bond representing a C_s structure for CH_5^+ could be formed among any pair of H atoms in CH_5^+. For $CH_5^+(H_2)$, the 3c2e bond was more or less localized around the H atom of the CH_5^+ core which was complexed by the H_2 molecule. Scrambling through the two internal motions (via s-C_s and C_{2v} structures) were still expected to be significant. For $CH_5^+(H_2)_2$, the 3c2e bond was localized to the two H atoms which were bound by the two H_2 molecules. It was explained by the electron deficiency in the 3c2e bond which attracts the two H_2 molecules. Preference for the localized

3c2e bond was also predicted in the ab initio calculation at MP2/6-31G**, from the decrease in the angle of the 3c2e bond (∠H1CH2) from 48.4° for $CH_5^+(H_2)$ to 47.7° for $CH_5^+(H_2)_2$ (see Fig. 9A and 9B).[15] But, the scrambling through the CH_3 internal rotation was still extensive. For $CH_5^+(H_2)_3$, the CH_5^+ core was semi-rigid with the CH_3 internal rotation considerably hindered, but the in-plane wagging motion unhindered.

In the IR spectrum for the C-H stretching modes of $CH_5^+(H_2)$ (Fig. 5B), the center of the observed feature (2965 cm^{-1}) was only 23 and 27 cm^{-1} red-shifted from the average (2988 cm^{-1}) of the three highest ab initio C-H stretching frequencies of a C_s CH_5^+ (e-C_s and s-C_s), as shown in Table II, and the average C-H stretching frequency (2992 cm^{-1}) of CH_4, respectively. This result suggested that most of the structures possessed by the CH_5^+ core during the scrambling still contain a CH_3 unit with strong C-H bonds like those in the optimized C_s CH_5^+ structures or the C-H bonds in CH_4. The broad low frequency shoulder observed in the IR spectrum was suggestive of the scrambling through the in-plane wagging motion (via C_{2v} structure), which could allow the asymmetric CH_2 stretching mode of the 4c3e bond in C_{2v} CH_5^+ (2732 cm^{-1}) to contribute to the low frequency feature. Therefore, the CH_5^+ core in $CH_5^+(H_2)$ continues to scramble through the CH_3 internal rotation and the in-plane wagging motion, but the C-H bonds which are not directly involved in the nonclassical bond (3c2e or 4c3e bond), are expected to be strong like the C-H's in CH_4. The A-type vibration-rotational transitions observed in the IR spectrum for the H-H stretching mode (Fig. 6A), suggested the structure of $CH_5^+(H_2)$ with the H_2 molecule weakly bound to one of the two H atoms forming the 3c2e bond, in good agreement with the theoretical predictions.[19] The anomalously intense peaks and the rotational fine features observed in the spectrum could be due to the scrambling motions involving the CH_3 internal rotation and in-plane wagging motion.

For $CH_5^+(H_2)_2$, one broad and intense peak at 2957 cm^{-1} and one narrow peak at 3078 cm^{-1}, were observed while the broad low frequency shoulder observed for $CH_5^+(H_2)$ was no longer present in the IR spectrum (Fig. 5C). This result was consistent with the theoretical prediction that the CH_5^+ core has a C_s structure with the 3c2e bond localized. The scrambling through the in-plane wagging motion (via C_{2v} structure) was expected to be considerably hindered. The broad feature at 2957 cm^{-1} suggested that the scrambling through the CH_3 internal rotation was still significant. Strong anharmonic couplings for the vibrational modes involving

the CH_3 group were also expected. The broad and intense peak at 2957 cm^{-1} could be assigned to the two strongly coupled C-H stretching modes, while the narrow feature at 3078 cm^{-1} could be due to the other less coupled C-H stretching mode. The A-type vibration-rotational transitions observed in the IR spectrum for the H-H stretching modes (Fig. 6B), were suggestive of the $CH_5^+(H_2)_2$ structure with the two H_2 molecules bound to the two H atoms forming the 3c2e bond in the CH_5^+ core. The in-phase vibration of the two H-H stretching modes would be exactly along the A-axis of the ion when the CH_3 internal rotation is free.

For $CH_5^+(H_2)_3$, three partially resolved features, centered at 2892, 2977, 3062 cm^{-1} were observed in the IR spectrum (Fig. 5D), indicating the semi-rigid nature of the CH_5^+ core. Only scrambling would occur through quantum tunneling, causing the broad bandwidths. It is interesting to notice that the observed frequencies (2892, 2977, 3062 cm^{-1}) match well with the three ab initio CH_3 stretching frequencies, for e-C_s CH_5^+ (2891, 2993, 3079 cm^{-1})[11] and e-C_s $CH_5^+(H_2)$ (2898, 2998, 3081 cm^{-1}).[19] It suggests that the CH_5^+ core in $CH_5^+(H_2)_3$ possesses an e-C_s structure. Correspondingly, the three C-H stretching frequencies could be assigned to the symmetric CH_3 breathing, symmetric CH_3 degenerate stretching, and asymmetric CH_3 stretching modes of e-C_s CH_5^+ core in $CH_5^+(H_2)_3$. The ab initio MD simulation also predicted the semi-rigid nature of the CH_5^+ core, but predicted the scrambling through the in-plane wagging motion, different from the experimental result. The difference was attributed to the underestimation of the potential barrier for the in-plane wagging motion. In addition, other isomers of $CH_5^+(H_2)_3$ such as the structure with the third H_2 located out of plane to the 3c2e bond, may contribute to the observed IR spectrum.

For $CH_5^+(H_2)_4$, three resolved features, centered at 2878, 2979, and 3067 cm^{-1}, were observed in the IR spectrum (Fig. 5E), similar to the spectral features observed for $CH_5^+(H_2)_3$ (Fig. 5D). This result suggested that the scrambling of CH_5^+ core was more or less frozen out by the first three H_2 molecules, and the addition of the fourth H_2 molecule resulted in only a minor change in the structure of the CH_5^+ core. It was consistent with the results of Hiraoka and coworkers' measurements[15] on ΔH°_T's of the clustering reactions, $CH_5^+(H_2)_{n-1} + H_2 = CH_5^+(H_2)_n$ (see Table I), in that the stabilization of the cluster ions by the fourth H_2 molecule was small, compared to the stabilization by the third H_2 (0.17 vs 0.04 kcal/mole). In the IR spectrum for the H-H stretching modes of $CH_5^+(H_2)_4$ (Fig. 6D), the frequency shift of the observed feature from

the adjacent smaller cluster decreased from that for $CH_5^+(H_2)_3$, which was consistent with the trend for the C-H stretching modes as described above.

For $CH_5^+(H_2)_n$ (n=5,6), the trend of the spectral features observed in the IR spectrum (Fig. 5F, 6E, 6F), were similar to the case for $CH_5^+(H_2)_4$. The structures of the CH_5^+ cores were expected to be unchanged by the fifth and sixth H_2 molecules.

4.2 Stabilities and structures of $CH_5^+(H_2)_n$ (n=1-6)

In this section, the stabilities of the solvated complexes, $CH_5^+(H_2)_n$ (n=1-6) are discussed from the correlation between the H-H stretching frequencies and the strength of the interactions. Possible solvation structures are also presented.

As described previously, the interactions between CH_5^+ core and the H_2 molecules are dominated by the electrostatic charge-induced dipole interactions, where the strengths are proportional to the charge densities at the H atoms of CH_5^+ core, the binding sites for the H_2 molecules in $CH_5^+(H_2)_n$ (n=1-6). The effect of the electrostatic interaction on the vibrational frequency of the solvent H_2 molecule has been addressed previously in the calculation of the Stark shifts of the H-H stretching modes as a function of the distance from the charge to H_2 molecule by Hunt and Poll.[30] The frequency shifts of the H-H stretching modes from free H_2 could be a measure of the strength of the electrostatic interactions. Fig. 7 shows a plot of the peak positions of the H-H stretching modes as a function of the size of the clusters. The frequency shifts from free H_2 (4160 cm^{-1}) decreased as the number of H_2 molecules increased, and reached a limit at n=4. This result clearly indicated that the positive charge of the CH_5^+ core was gradually delocalized as the size of the clusters increased.

Fig. 8 shows a plot of the correlation between the H-H stretching frequencies and the $-\Delta H^\circ_T$'s of the clustering reactions, $CH_5^+(H_2)_{n-1} + H_2 = CH_5^+(H_2)_n$ (n=1-4), measured by Hiraoka and coworkers (see Table I).[15] The correlation followed the idea of the previous work by Hunt and Poll as described above. A good correlation was found between the H-H stretching frequencies and the $-\Delta H^\circ_T$'s of the clustering reactions, as shown in Fig. 8. From the correlation, the $-\Delta H^\circ_T$'s for the formation of $CH_5^+(H_2)_5$ and $CH_5^+(H_2)_6$, which were not measured in the previous work by Hiraoka and coworkers, were calculated to be 1.52 and 1.49 kcal/mole, respectively. Furthermore, one could correlate the H-H stretching frequencies with the theoretical

binding energies to test the consistency of the calculations.

Finally, it is appropriate to address the possible structures of the solvated complexes, $CH_5^+(H_2)_n$ (n=1-6) by combining the results of this work and the results of the theoretical work. Fig. 9 shows the possible structures of $CH_5^+(H_2)_n$ (n=1-6). Both experimental and theoretical results[15,19] consistently suggested the structures shown in Fig. 9A and 9B for $CH_5^+(H_2)$ and $CH_5^+(H_2)_2$, where the H_2 molecules were bound to the H atoms forming the 3c2e bond in the CH_5^+ core. For $CH_5^+(H_2)_3$, the most stable structure was predicted to be the structure shown in Fig. 9C, but other structures such as the structure shown in Fig. 9D, where the third H_2 was located out of plane to the 3c2e bond, could be formed in internally hot ions. Due to the weak interactions between the CH_5^+ core and the H_2 molecules in $CH_5^+(H_2)_n$ (n≥4), the structures of the ions are better described as the mixture of several structures undergoing rapid isomerizations on the very shallow potential energy surfaces. But, it is still instructive to consider the local minimum energy structures for $CH_5^+(H_2)_n$ (n≥4). For $CH_5^+(H_2)_4$, the fourth H_2 could bind to either the H4 (or H5) of the CH_5^+ core (Fig. 9E) or the 3c2e bond in the out-of-plane fashion (Fig. 9F). For $CH_5^+(H_2)_5$, the fifth H_2 molecule could bind to the H5 (or H4) of the CH_5^+ core; completing the first solvation shell around the CH_5^+ core (Fig. 9G). In addition, the $CH_5^+(H_2)_5$ ions could form the structures with one or two H_2 molecules binding to the 3c2e bond in the out-of-plane fashion (Fig. 9H). For $CH_5^+(H_2)_6$, the sixth H_2 molecule can bind to the 3c2e bond of the CH_5^+ core in the out-of-plane fashion (Fig. 9I) after the first solvation shell is complete at n=5. Other structures involving the isomers of $CH_5^+(H_2)_4$ and $CH_5^+(H_2)_5$ are also possible for $CH_5^+(H_2)_6$.

5. SUMMARY

The infrared spectra for the molecular hydrogen-solvated carbonium ions, $CH_5^+(H_2)_n$ (n=1-6) have been presented. Spectroscopic evidence has been presented in support of the scrambling of CH_5^+ through the large amplitude motions such as the CH_3 internal rotation and the in-plane wagging motion. More importantly, the scrambling motions of CH_5^+ cores were slowed down by attaching the solvent H_2 molecules to the core ion. The complete freezing of the scrambling motions was found when the first three H_2 molecules were bound to the CH_5^+ core. A good agreement between the experimental results and the theoretical predictions was found in the dynamics of CH_5^+.

A clear extension of this work would be to improve the resolution of the IR spectra for the H-H stretching modes of $CH_5^+(H_2)$ and $CH_5^+(H_2)_2$, which would provide additional information on the structures and the rotational and tunneling dynamics of both the CH_5^+ cores and the entire clusters. High order overtone transitions of free CH_5^+ can be measured by improving the schemes for vibrational excitation and probe with the use of high power IR and CO_2 lasers. In addition, significant efforts for the generation of internally cold CH_5^+ ions should be made, so that the IR spectra are not smeared out due to spectral congestion by the scrambling of CH_5^+.

ACKNOWLEDGEMENT

We would like to thank Dr. John T. Tse at National Research Council (NRC) of Canada, for providing us with the results of his calculation prior to publication. This work was supported by the Director, Office of Energy Research, Office of Basic Energy Sciences, Chemical Sciences Division of the U.S. Department of Energy under Contract No. DE-AC03-76SF00098.

REFERENCES

1. G.A. Olah, G.K.S. Prakash, and J. Sommer, Superacids (Wiley-Interscience, New York, 1985).

2. G.A. Olah, Carbocations and Electrophilic Reactions (Verlag Chemie, Weinheim, 1973).

3. F.H. Field, Acc. Chem. Res., v.1, 42 (1968); F.H. Field, and M.S.B. Munson, J. Am. Chem. Soc., v. 87, 3289 (1965).

4. G.A. Olah, G. Klopman, and R.H. Schlosberg, J. Am. Chem. Soc., v.91, 3261 (1969); G.A. Olah and R.H. Schlosberg, J. Am. Chem. Soc., v.90, 2726 (1968).

5. D.P. Stevenson and D.O. Schissler, J. Chem. Phys., v.23, 1353 (1955).

6. A. Dalgano, in Molecular Astrophysics, edited by G.H.F. Dierchsen et al (D. Reidel Publishing Company, 1985) pp 3-22.

7. V. Dyczmons, V. Staemmler, and W. Kutzelnigg, Chem. Phys. Lett., v.5, 361 (1970).

8. W.A. Lathan, W.J. Hehre, L.A. Curtiss, and J.A. Pople, J. Am. Chem. Soc., v.93, 6377 (1971); K. Ragavachari, R.A. Whiteside, J.A. Pople, and P.v.R. Schleyer, J. Am. Chem. Soc., v.103, 5649 (1981).

9. K. Hirao and S. Yamabe, Chem Phys., v.89, 237 (1984).

10. W. Klopper and W. Kutzelnigg, J. Phys. Chem., v.94, 5625 (1990).

11. P.R. Schreiner, S.J. Kim, H.F. Schaefer, and P.v.R. Schleyer, J. Chem. Phys., v.99, 3716 (1993).

12. P.v.R. Schleyer and J.W.M. Carneiro, J. Comput. Chem., v.13, 997 (1992).

13. G.E. Scuseria, Nature, v.366, 512 (1993).

14. K. Hiraoka and T. Mori, Chem. Phys. Lett., v.161, 111 (1989); K. Hiraoka and P. Kebarle, J. Am. Chem. Soc., v.97, 4179 (1975).

15. K. Hiraoka, I. Kudaka, and S. Yamabe, Chem. Phys. Lett., v.184, 271 (1991).

16. M.D. Sefcik, J.M.S. Henis, and P.P. Gasper, J. Chem. Phys., v.61, 4321 (1974).

17. R.D. Smith and J.H. Futrell, Chem. Phys. Lett., v.36, 545 (1975).

18. A.J.R. Heck, L.J. de Koning, and N.M.M. Nibbering, J. Am. Soc. Mass Spectrom., v.2, 453 (1991).

19. S.J. Kim, P.R. Schreiner, P.v.R. Schleyer, and H.F. Schaefer, J. Phys. Chem., v.97, 12232 (1993).

20. D.W. Boo and Y.T. Lee, Chem. Phys. Lett., v.211, 358 (1993).

21. D.W. Boo, Z.F. Liu, J.T. Tse, Y.T. Lee, and A.G. Suits, submitted to Science (1995).

22. S.W. Bustamente, Ph.D. Thesis, University of California at Berkeley (1983).

23. M. Okumura, Ph.D. Thesis, University of California at Berkeley (1986).

24. L.I.-C. Yeh, Ph.D. Thesis, University of California at Berkeley (1988).

25. J.M. Price, Ph.D. Thesis, University of California at Berkeley (1991).

26. D.W. Boo, Ph.D. Thesis, University of California at Berkeley (1995).

27. R.N. Daly, Rev. Sci. Instr., v.31, 264 (1960).

28. G. Herzberg, Molecular Spectra and Molecular Structure, v.II Infrared and Raman Spectra of Polyatomic Molecules (Krieger Publishing Company, Florida, 1991).

29. J.T. Tse, unpublished results.

30. J.L. Hunt and J.D. Poll, Can. J. Chem., v.63, 84 (1985).

TABLE I. Experimental and theoretical dissociation energies and enthalpies for $CH_5^+(H_2)_n$ (Units are kcal/mole)

reference		n = 1	2	3	4
Hiraoka et al.[a]	$-\Delta H^\circ_T$	1.88±0.10	1.78±0.10	1.61±0.10	1.57±0.10
Hiraoka et al.[a] MP2/6-31G**	D_e	2.02	1.76	0.91	0.64
Schaefer et al.[b] TZ2P+d CCSD(T)	$D_e(D_o)$	3.48(1.46)			

[a]Ref. 15.
[b]Ref. 19.

TABLE II. Vibrational frequencies[a] of the C-H and H-H stretching modes for $CH_5^+(H_2)_n$ (n=1- 3) predicted by the ab initio calculations. Units are in cm^{-1}.

	Asym CH_3 stretch	Sym CH_3 deg stretch	Sym CH_3 breath	H_2 stretch
CH_5^+, e-C_s TZ2P+f[b] CCSD	3079(3063)	2993(2977)	2898(2883)	-
CH_5^+, s-C_s TZ2P+f[b] CCSD	2968(2952)	3085(3069)	2914(2898)	-
CH_5^+, C_{2v} TZ2P+f[b†] CCSD	3094(3077)	2987(2971)	2732(2717)	-
$CH_5^+(H_2)$, e-C_s CH_5^+ TZ2P CCSD[c]	3081(3059)	2998(2977)	2898(2878)	4107(4078)
$CH_5^+(H_2)$ C_{2v} CH_5^+ TZ2P SCF[c†]	3079(3063)	2972(2956)	2706(2692)	4104(4082)
$CH_5^+(H_2)_2$ e-C_s CH_5^+ MP2/6-311G(D,P)[d]	3278(3069)	3183(2980)	3068(2872)	4446(4162) 4463(4178)
$CH_5^+(H_2)_3$ e-C_s CH_5^+ MP2/6-311G(D,P)[d]	3280(3071)	3180(2977)	3043(2849)	4448(4164) 4459(4174) 4493(4206)

[a]The numbers in parenthesis are the frequencies scaled by the ratio of 2977 cm^{-1}, one of the observed peaks for $CH_5^+(H_2)_3$, and the corresponding ab initio C-H stretching frequency for the eclipsed C_s CH_5^+ core at the level of theory. For example, the ratio was 2977/2993=.995 at TZ2P+f CCSD; 2977/2998=.993 at TZ2P CCSD; 2977/2993=.995 at TZ2P SCF; 2977/3180=.936 at MP2/6-311G(D,P).

[b]Ref. 11. [c]Ref. 19. [d]Ref. 29.

[†]Note that the vibrational assignments for C_{2v} CH_5^+ should be changed to the CH_2 asymmetric, CH_2 symmetric, and CH_2^* asymmetric stretching modes, respectively (CH_2^* indicates the two of three C-H bonds forming the 4c3e bond).

TABLE III. Vibrational frequencies of the molecular hydrogen solvated carbonium ions. Units are in cm^{-1}.

Ions	C-H Stretching Modes[a]	Band Origins of H-H Stretching Modes
$CH_5^+(H_2)$	2964(2907,2965,3070)[b]	4077.4[c]
$CH_5^+(H_2)_2$	2957(2930,2983),[b] 3078	4088.2[c]
$CH_5^+(H_2)_3$	2892,2977,3062	4099[d]
$CH_5^+(H_2)_4$	2878,2979,3067	4106[d]
$CH_5^+(H_2)_5$	2879,2972,3043	4109[d]
$CH_5^+(H_2)_6$	N.O.[e]	4111[d]

[a]These C-H stretching frequencies were determined by a least squares fit with three gaussian peaks.
[b]These frequencies in parantheses were not resolved in the observed spectra. The frequencies in parenthesis for n=2 were obtained by fitting with two equal gaussian peaks.
[c]These frequencies were measured at the maximum of the Q-branches.
[d]These frequencies were measured at the center of the observed features.
[e]Not Observed.

FIGURE CAPTIONS

Fig. 1 Ab initio structures of CH_5^+.

Fig. 2 Schematic of the experimental apparatus. (A) corona discharge source; (B) skimmer and cone extractor; (C) electrostatic lenses; (D) plates separating two differential pumping regions; (E) quadrupole lens pair; (F) sector magnet; (G) quadrupole bending field; (H) deceleration field; (I) octapole ion trap; (J) quadrupole mass filter; (K) a Daly ion detector; (L) electronmultiplier tube.

Fig. 3 Schematic of the corona discharge ion source used in this work.

Fig. 4 Mass spectrum showing the carbonium ion CH_5^+ and the molecular hydrogen solvated carbonium ions $CH_5^+(H_2)_n$ (n=1-6). The mixing ratio of CH_4:H_2 was 1:3,000,000, and the source temperature and the discharge current were -30°C and 20μA, respectively.

Fig. 5 IR spectra for the C-H stretching modes of the CH_5^+ cores: (A) $CH_5^+(H_2)$, under hot ion conditions; (B) $CH_5^+(H_2)$, under cold ion conditions; (C) $CH_5^+(H_2)_2$; (D) $CH_5^+(H_2)_3$; (E) $CH_5^+(H_2)_4$; (F) $CH_5^+(H_2)_5$.

Fig. 6 IR spectra for the H-H stretching modes of the solvent H_2 molecules: (A) $CH_5^+(H_2)$; (B) $CH_5^+(H_2)_2$; (C) $CH_5^+(H_2)_3$; (D) $CH_5^+(H_2)_4$; (E) $CH_5^+(H_2)_5$; (F) $CH_5^+(H_2)_6$.

Fig. 7 Plot of the H-H stretching frequencies as a function of the size of the clusters $CH_5^+(H_2)_n$ (n=1-6).

Fig. 8 Plot of correlation between the H-H stretching frequencies and the $-\Delta H^\circ_T$'s of the clustering reactions, $CH_5^+(H_2)_{n-1} + H_2 = CH_5^+(H_2)_n$ (n=1-4).

Fig. 9 Possible structures of the molecular hydrogen solvated carbonium ions, $CH_5^+(H_2)_n$ (n=1-6).

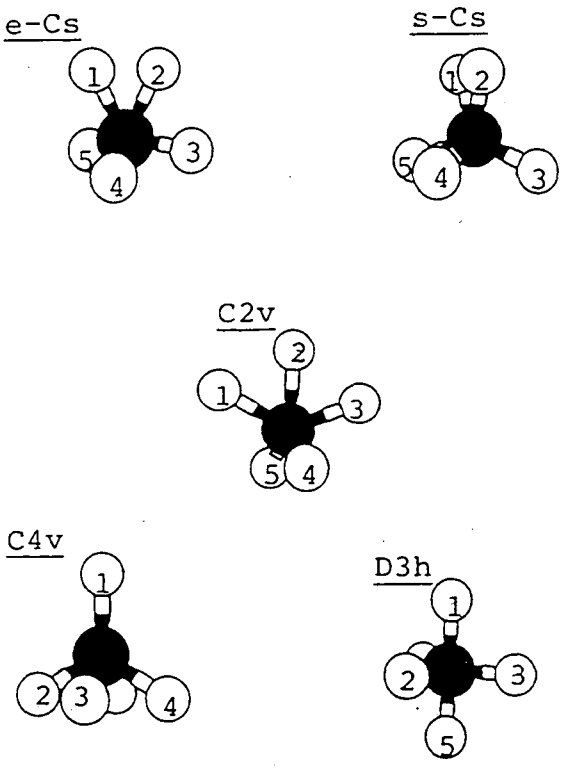

Fig. 1

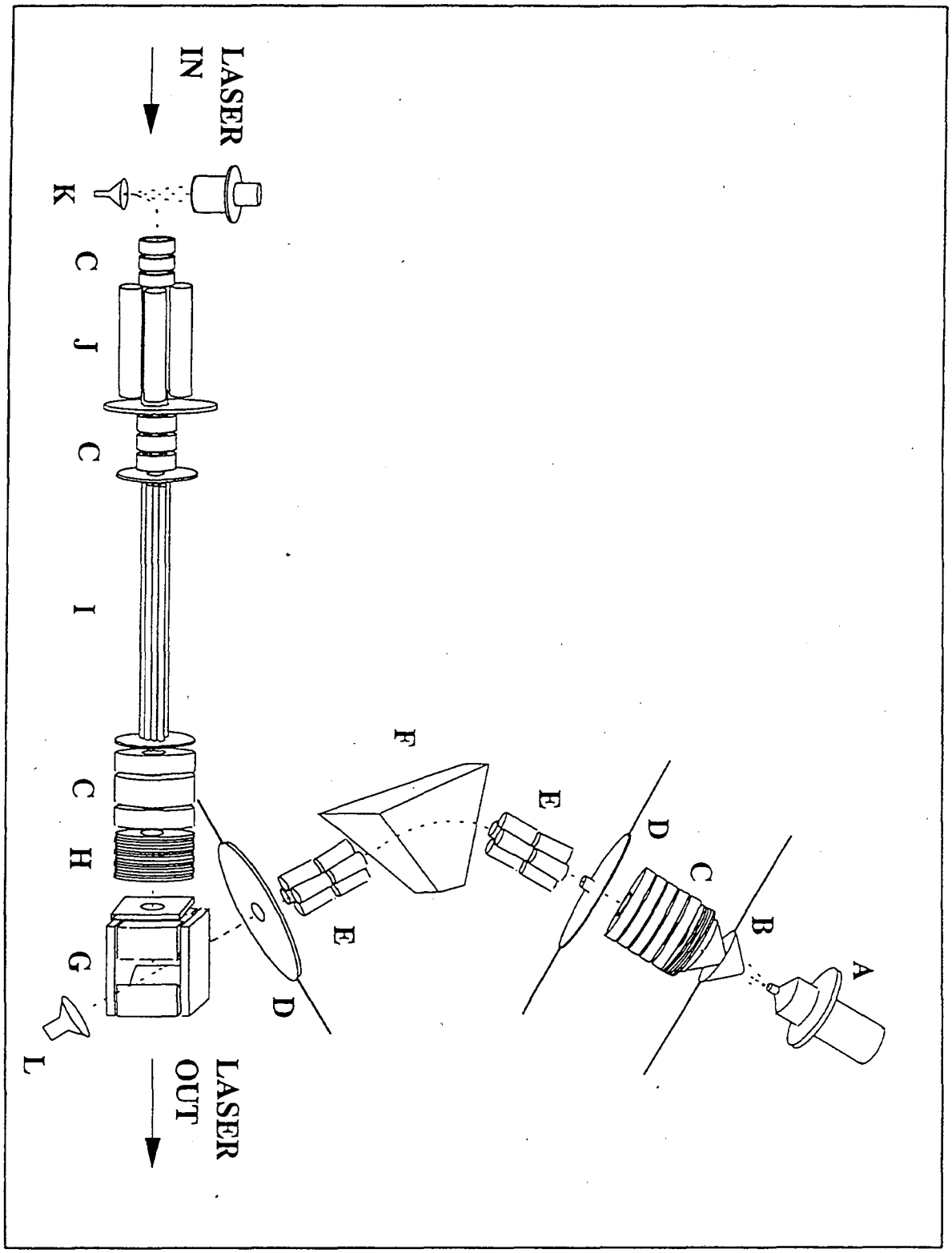

Fig. 2

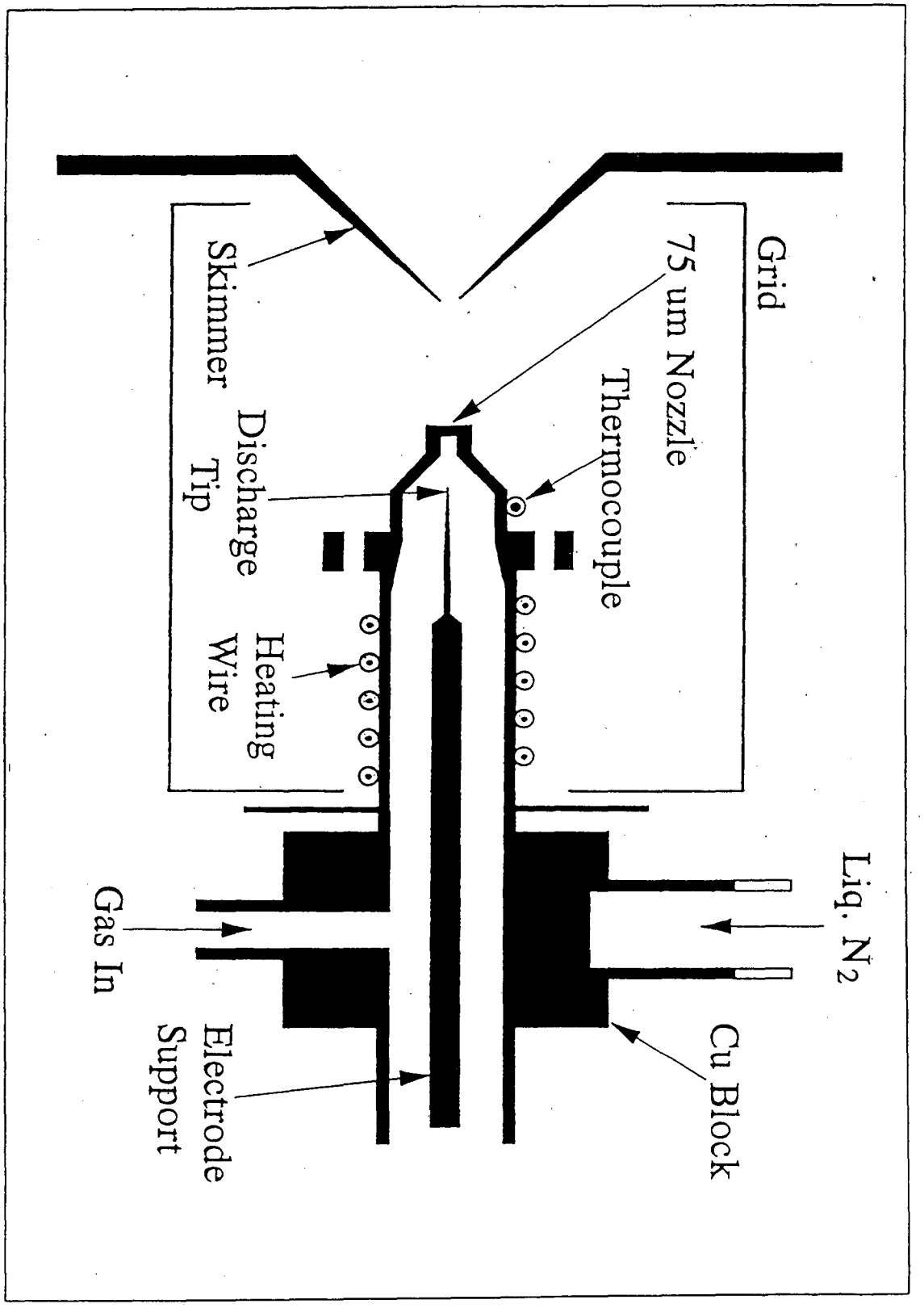
Grid
75 um Nozzle
Thermocouple
Skimmer
Discharge Tip
Heating Wire
Liq. N_2
Gas In
Electrode Support
Cu Block

Fig. 3

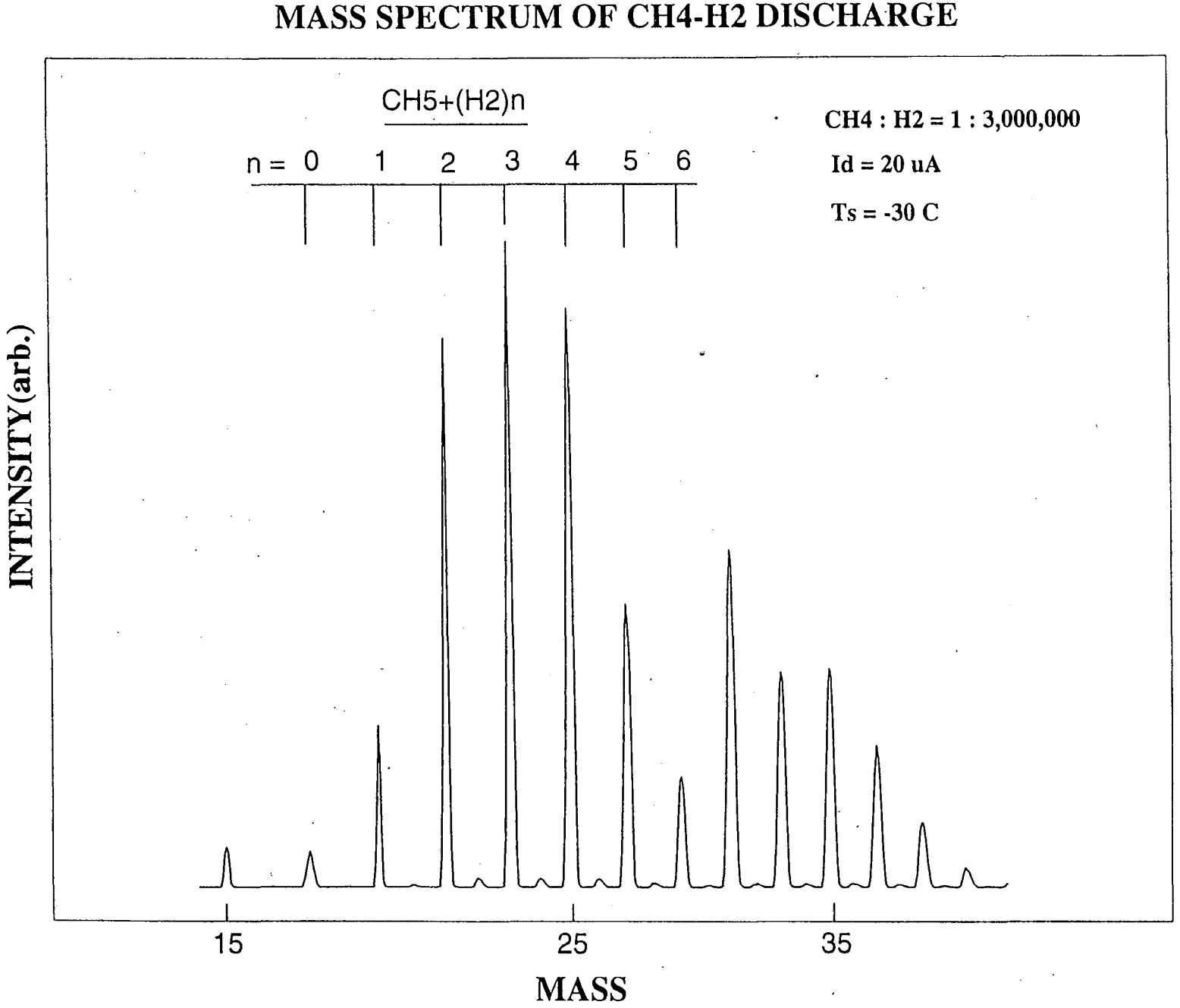
MASS SPECTRUM OF CH4-H2 DISCHARGE
CH5+(H2)n
n = 0 1 2 3 4 5 6
CH4 : H2 = 1 : 3,000,000
Id = 20 uA
Ts = -30 C
INTENSITY(arb.)
15
25
35
MASS

Fig. 4

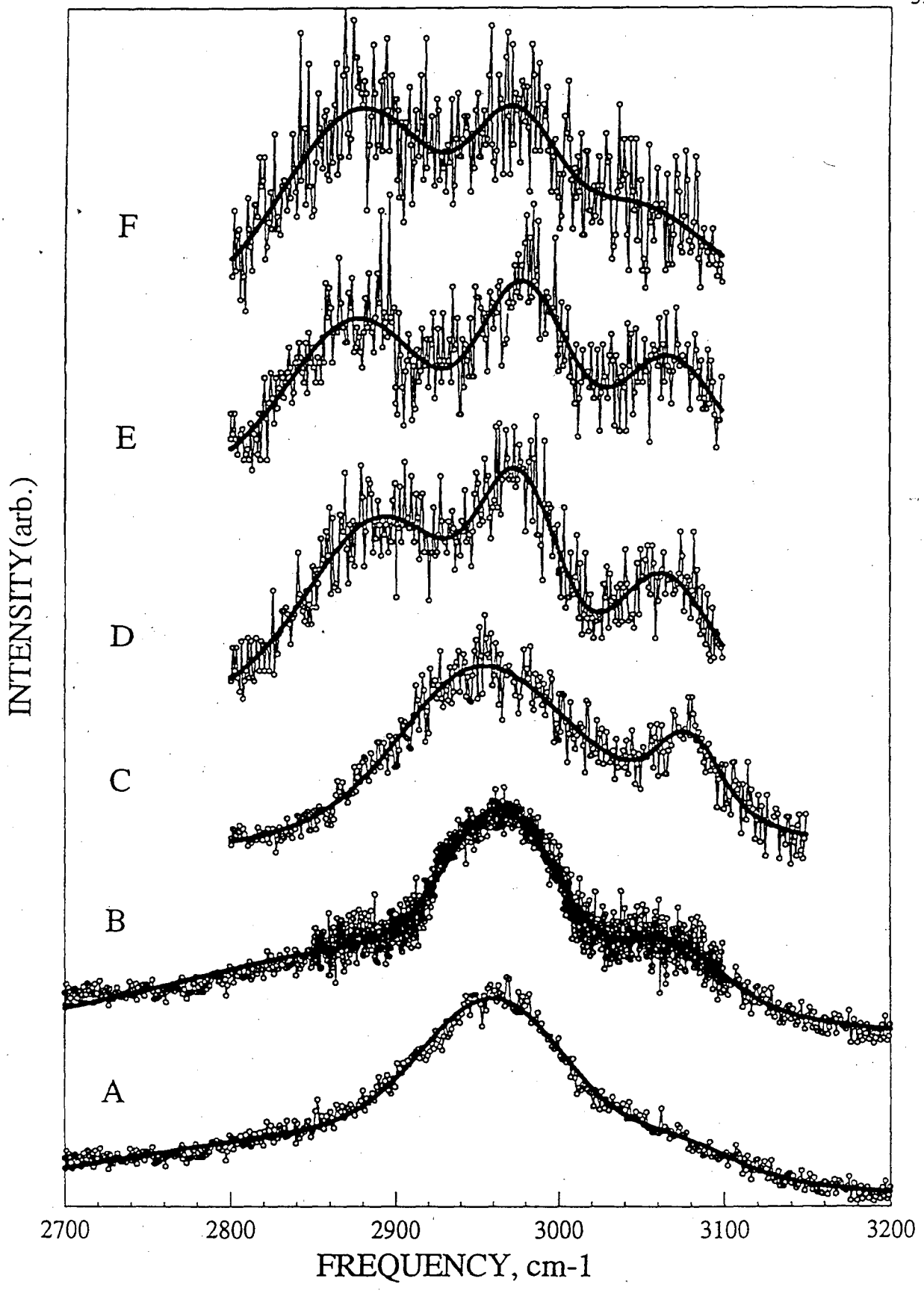
F
E
D
C
B
A
INTENSITY(arb.)
2700
2800
2900
3000
3100
3200
FREQUENCY, cm-1

Fig. 5

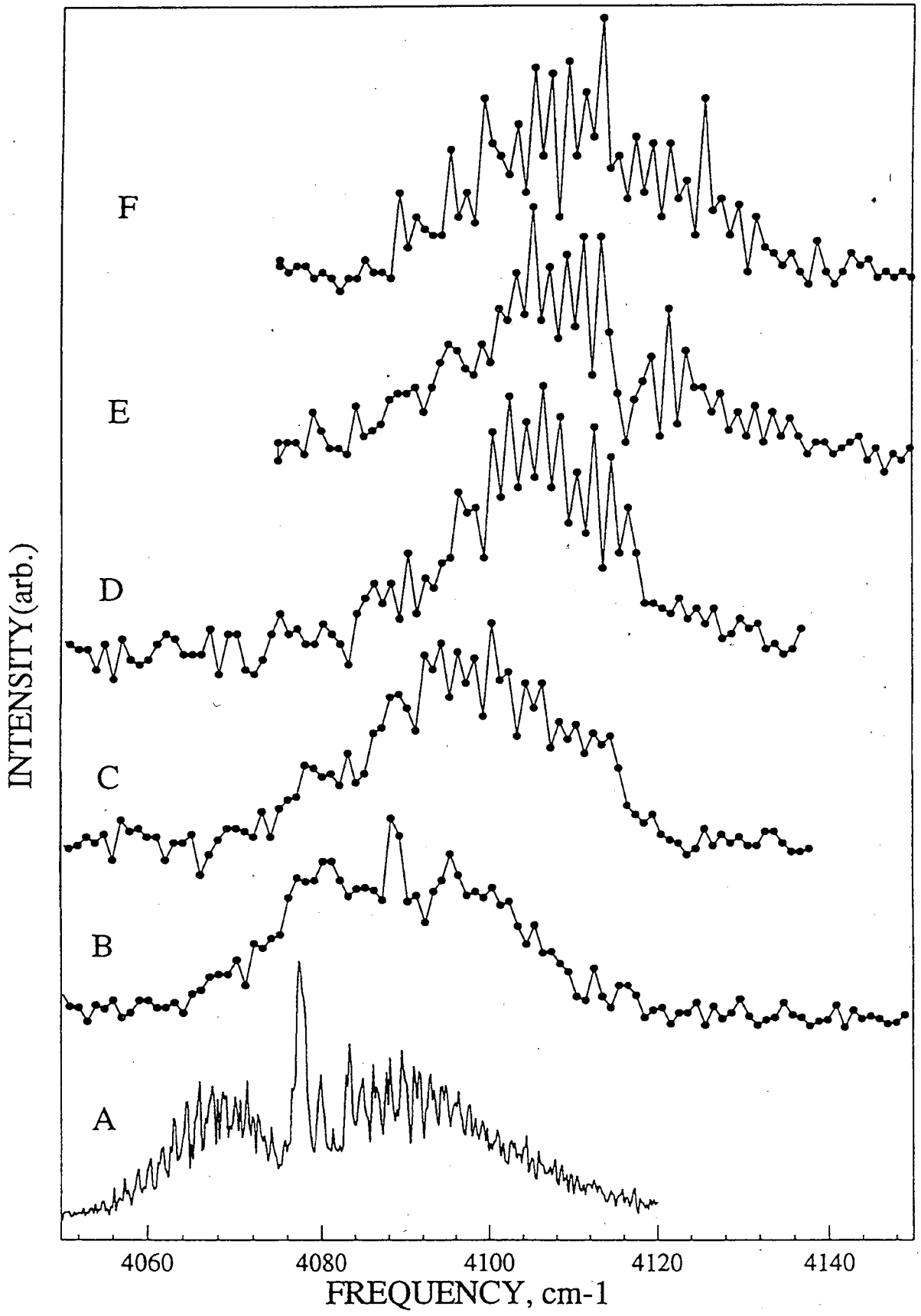
F
E
D
C
B
A
INTENSITY(arb.)
4060
4080
4100
4120
4140
FREQUENCY, cm-1

Fig. 6

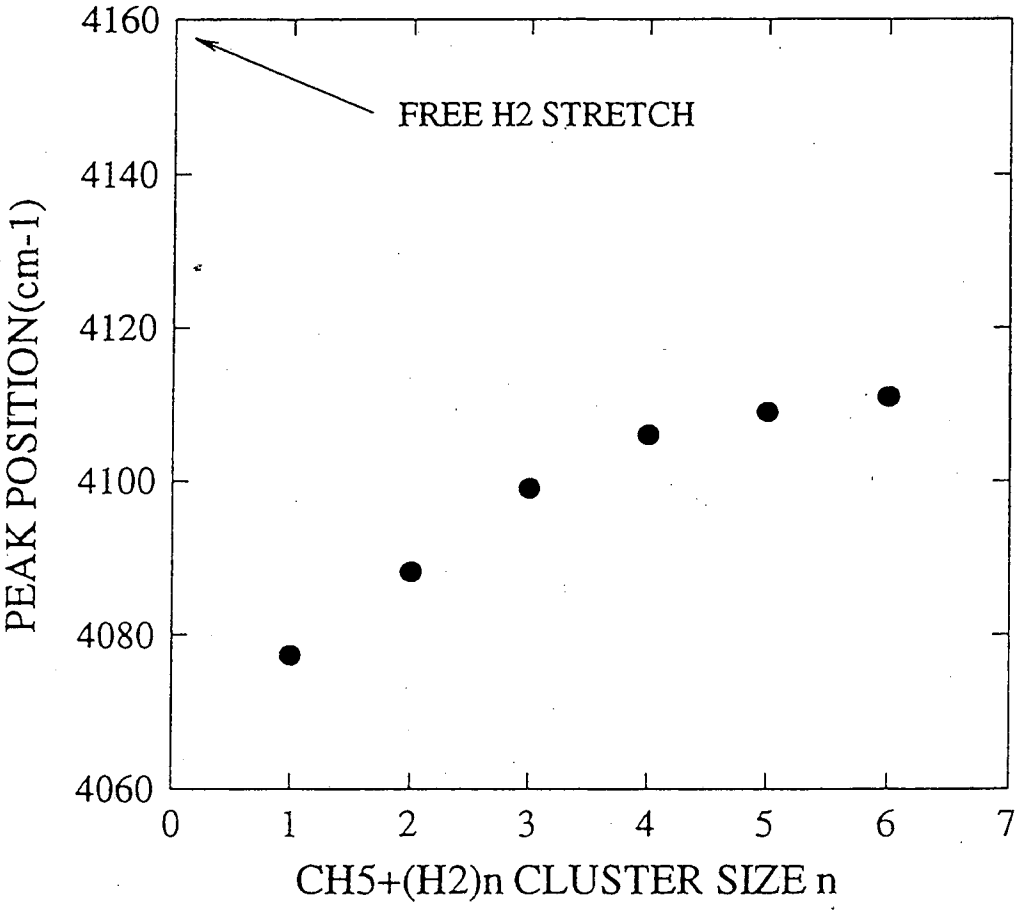
4160
4140
4120
4100
4080
4060
PEAK POSITION(cm-1)
FREE H2 STRETCH
0
1
2
3
4
5
6
7
CH5+(H2)n CLUSTER SIZE n

Fig. 7

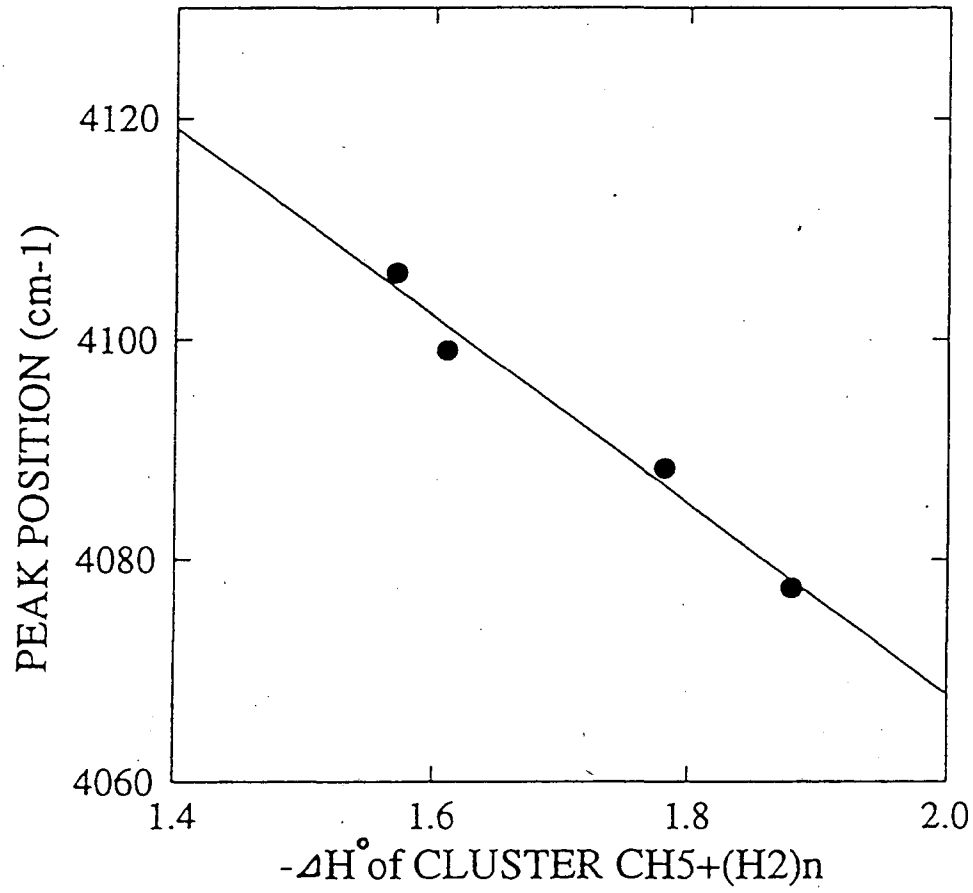
4120
4100
4080
4060
PEAK POSITION (cm-1)
1.4
1.6
1.8
2.0
-ΔH°of CLUSTER CH5+(H2)n

Fig. 8

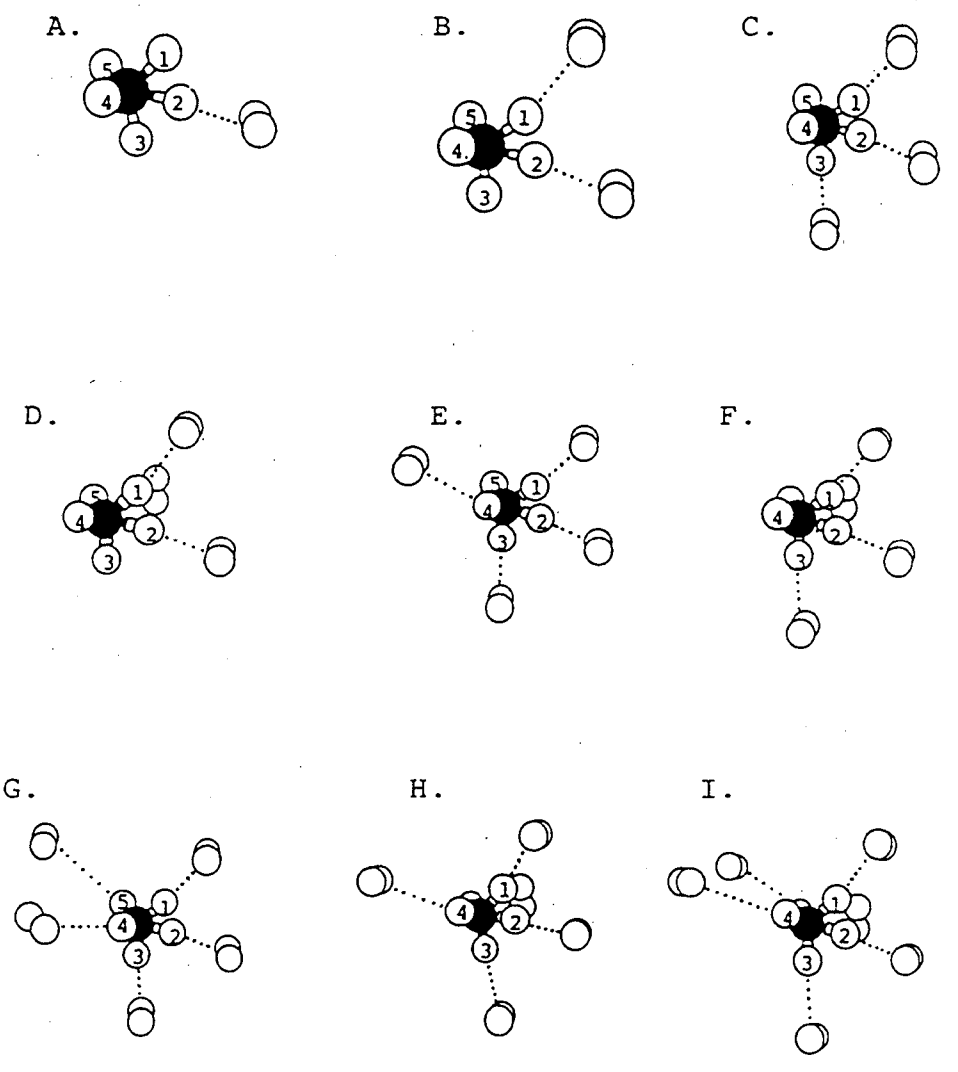

Fig. 9

LAWRENCE BERKELEY LABORATORY
UNIVERSITY OF CALIFORNIA
TECHNICAL INFORMATION DEPARTMENT
BERKELEY, CALIFORNIA 94720